

This work has been submitted to the IEEE for possible publication. Copyright may be transferred without notice, after which this version may no longer be accessible.

arXiv:2603.08962v1 [cs.IT] 9 Mar 2026

Mitigation of UE Antenna Calibration Errors via Differential STBC in Cell-Free Massive MIMO

Marx M. M. Freitas, *Member, IEEE* and Stefano Buzzi, *Fellow, IEEE*

Abstract—This letter investigates the use of differential space-time block coding (DSTBC) to address antenna array calibration impairments at multi-antenna user equipment (UE) in the downlink (DL) of cell-free massive MIMO (CF-mMIMO) systems. We show that, by exploiting DSTBC, reliable DL communication can be achieved without explicit UE-side calibration or channel phase knowledge. Simulation results demonstrate that the proposed DSTBC-based transmission effectively mitigates the impact of antenna-dependent phase offsets, restoring near-coherent performance in CF-mMIMO networks.

Index Terms—Antenna calibration, cell-free massive MIMO networks, differential space-time block coding, non-reciprocity.

I. INTRODUCTION

User-centric (UC) cell-free massive multiple-input multiple-output (CF-mMIMO) systems are widely regarded as a key enabling technology for next-generation wireless networks [1]. Recent CF-mMIMO research increasingly focuses on practical hardware impairments, which can severely limit performance if not properly handled. Among these investigations, non-ideal radio frequency (RF) chains, whose transmitreceive asymmetries violate the channel reciprocity assumption underpinning time-division duplex (TDD) operation [2], are one of the most considered and investigated. Although the wireless channel is reciprocal, hardware distortions create unknown phase and amplitude offsets that conventional precoding techniques cannot remove, degrading coherent downlink (DL) transmission. To address this, intra- and inter-access point (AP) antenna calibration schemes have been proposed [3], [4], assuming single-antenna user equipments (UEs). These papers address only impairments from the APs' RF chains and ignore hardware imperfections at the UE side.

The performance of CF-mMIMO systems further improves when UEs have multiple antennas, enabling multiple spatial data streams and providing extra array and multiplexing gains [5]–[7]. Hence, antenna calibration at the UE side is also relevant. While over-the-air (OTA) calibration is feasible for fixed, network-controlled APs, applying it to mobile UEs is inherently challenging. Therefore, this letter studies the unexplored impact of antenna calibration impairments at multi-antenna UEs in the DL of CF-mMIMO. Unlike our previous

contribution [8], which focused on mitigating phase misalignments among distributed APs, we show here that differential space-time block coding (DSTBC) can be also used to overcome channel non-reciprocity caused by unknown, time-varying phase offsets in the UEs' RF chains, without explicit calibration or phase estimation. Numerical results show that the proposed approach significantly improves bit-error rate (BER) and spectral efficiency (SE), and recovers near-coherent DL performance despite UE-side calibration errors.

This letter is organized as follows. Section II describes the system model and its mathematical formulation under channel non-reciprocity. Section III presents the adaptation of DSTBC schemes to CF-mMIMO systems with multi-antenna UEs and non-reciprocal channels. Section IV shows numerical results, while, finally, Section V wraps up the letter.

II. SYSTEM MODEL AND PROBLEM STATEMENT

We consider a standard CF-mMIMO system with L APs and K UEs. Each AP has N_{AP} antennas and each UE has N_{UE} antennas. The APs are connected to a central processing unit (CPU) by error-free fronthaul links, and the system operates in TDD mode. The uplink (UL) on-air channel from UE k to AP l is $\mathbf{G}_{k,l} = \beta_{k,l}^{1/2} \mathbf{H}_{k,l}$, where $\beta_{k,l}$ is the large-scale fading coefficient (path-loss and shadowing), and $\mathbf{H}_{k,l} \in \mathbb{C}^{N_{\text{AP}} \times N_{\text{UE}}}$ has independent and identically distributed (i.i.d) entries distributed as complex Gaussian $\mathcal{N}_{\mathbb{C}}(0, 1)$ ¹. By channel reciprocity, the DL on-air channel from AP l to UE k is $\mathbf{G}_{k,l}^{\text{H}}$. This common assumption allows channel estimation to be done only in the UL, with the estimates reused for DL transmission within the coherence interval.

In practice, however, this assumption is not exact due to hardware non-idealities. As shown in Fig. 1, the effective channel between AP l and UE k includes the TX and RX RF branches of each antenna. These hardware-dependent distortions cause amplitude and phase mismatches that break channel reciprocity. They can be modeled through the diagonal matrices $\tilde{\Phi}_{rx,l}^{\text{AP}}, \tilde{\Phi}_{tx,l}^{\text{AP}} \in \mathbb{C}^{N_{\text{AP}} \times N_{\text{AP}}}$ and $\tilde{\Phi}_{rx,k}^{\text{UE}}, \tilde{\Phi}_{tx,k}^{\text{UE}} \in \mathbb{C}^{N_{\text{UE}} \times N_{\text{UE}}}$, whose m -th diagonal elements are the coefficients $\phi_{rx,l}^m, \phi_{tx,l}^m$ (at AP l) and $\tilde{\phi}_{rx,k}^m, \tilde{\phi}_{tx,k}^m$ (at UE k), respectively. Consequently, the true UL and DL channels between the AP l and UE k , within the same coherence block, are:

$$\tilde{\mathbf{G}}_{k,l}^{\text{UL}} = \tilde{\Phi}_{rx,l}^{\text{AP}} \mathbf{G}_{k,l} \tilde{\Phi}_{tx,k}^{\text{UE}}, \quad \tilde{\mathbf{G}}_{k,l}^{\text{DL}} = \tilde{\Phi}_{rx,k}^{\text{UE}} \mathbf{G}_{k,l}^{\text{H}} \tilde{\Phi}_{tx,l}^{\text{AP}}. \quad (1)$$

Clearly, we have that $\tilde{\mathbf{G}}_{k,l}^{\text{UL}} \neq [\tilde{\mathbf{G}}_{k,l}^{\text{DL}}]^{\text{H}}$ as the uncalibrated antenna arrays have destroyed the UL/DL channel reciprocity. In this letter, these hardware-induced matrices are assumed to be

This work was supported by the EU under the Italian National Recovery and Resilience Plan (NRRP) of NextGenerationEU, partnership on “Telecommunications of the Future” (PE00000001 - program “RESTART”), Structural Project NTN, Cascade Call INFINITE, CUP D93C22000910001.

The authors are with the Dept. of Electrical and Information Engineering (DIEI), University of Cassino and Southern Lazio, 03043 Cassino, Italy (e-mail: {marxmiguelmiranda.defreitas; buzzi}@unicas.it). S. Buzzi is also with the Consorzio Nazionale Interuniversitario per le Telecomunicazioni (CNIT), 43124 Parma, Italy.

¹ $\mathcal{N}_{\mathbb{C}}(\mu, \sigma^2)$ denotes a complex Gaussian random variable with mean μ and variance σ^2 , and $\mathbb{E}\{\cdot\}$ denotes expectation.

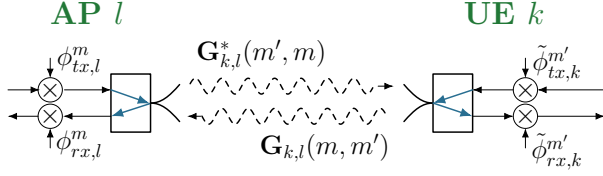


Fig. 1: Channel non-reciprocity effects caused by hardware-induced complex-valued offsets between antenna m at AP l and antenna m' at UE k .

quasi-static over at least two consecutive DSTBC codewords, as RF impairments typically evolve on millisecond timescales, much slower than symbol durations.

To analyze the system impact of uncalibrated antenna arrays, we focus specifically on the UL training phase and the DL data transmission phases², with the UL channels being estimated via minimum mean square error (MMSE) estimation [3], [8]. The generic UE k is served by a subset of APs called AP cluster, denoted as $\mathcal{L}_k \subset \{1, \dots, L\}$. The AP-UE association policy is encoded in the binary variables $a_{k,l} \in \{0, 1\}$. Since UEs are equipped with multiple antennas, it is assumed that each UE receives $N_s \leq N_{UE}$ parallel data streams³. We denote by $\mathbf{W}_{k,l} \in \mathbb{C}^{N_{AP} \times N_{UE}}$ the precoder used at AP l to transmit data to UE k ; this precoder is built using the UL estimated channels. In the UE k , since no channel knowledge is available, the channel-independent decoding matrix $\mathbf{M}_k = \mathbf{I}_{N_s} \otimes \mathbf{1}_{N_{UE}/N_s} \in \mathbb{C}^{N_{UE} \times N_s}$, introduced in [5], is used, with \otimes denoting kronecker product. Leaving $\mathbf{s}_i^p \in \mathbb{C}^{N_s \times 1}$ be the complex information symbols of the unit-norm intended for UE i at a discrete time epoch p , the signal received at UE k at time p can be expressed as

$$\tilde{\mathbf{y}}_k^p = \sum_{l=1}^L \sum_{i=1}^K a_{i,l} \tilde{\mathbf{G}}_{k,l}^{\text{DL}} \mathbf{W}_{i,l} \mathbf{M}_i \mathbf{s}_i^p + \mathbf{n}_k^p, \quad (2)$$

with $\mathbf{n}_k^p \in \mathbb{C}^{N_{UE} \times 1}$ representing the receiver noise. As to the precoding matrix $\mathbf{W}_{i,l}$, one possible choice is:

$$\mathbf{W}_{k,l}^{\text{ZISI}} = \sqrt{\rho_{k,l}} \hat{\mathbf{G}}_{k,l}^{\text{UL}} ((\hat{\mathbf{G}}_{k,l}^{\text{UL}})^H \hat{\mathbf{G}}_{k,l}^{\text{UL}})^{-1}, \quad (3)$$

where $\hat{\mathbf{G}}_{k,l}^{\text{UL}} \in \mathbb{C}^{N_{AP} \times N_{UE}}$ is the estimated UL channel matrix, and $\rho_{k,l}$ is a proper scaling factor that will be specified later. As shown in [5], this beamformer eliminates inter-stream interference at each UE under perfect calibration and channel state information. We therefore refer to this locally computable precoder as zero inter-stream interference (ZISI). Given (2), a soft estimate of the data symbols \mathbf{s}_k^p is [5]:

$$\hat{\mathbf{s}}_k^p = \mathbf{M}_k^H \tilde{\mathbf{y}}_k^p. \quad (4)$$

Substituting (2) and (3) into (4), and assuming that the channel is perfectly estimated, after some manipulations, we obtain:

$$\hat{\mathbf{s}}_k^p = \sum_{l \in \mathcal{L}_k} \sqrt{\rho_{k,l}} \mathbf{M}_k^H \tilde{\mathbf{G}}_{k,l}^{\text{DL}} \tilde{\mathbf{G}}_{k,l}^{\text{UL}} [(\tilde{\mathbf{G}}_{k,l}^{\text{UL}})^H \tilde{\mathbf{G}}_{k,l}^{\text{UL}}]^{-1} \mathbf{M}_k \mathbf{s}_k^p + \mathbf{i}_k^p. \quad (5)$$

In (5), we have isolated the useful term, whereas all interference and additive noise affecting UE k have been grouped

²The impact of uncalibrated antenna arrays is less critical in the UL, because UL channel estimation incorporates their effects and enables their subsequent compensation during the data detection stage.

³For the sake of simplicity, it is assumed that the number of streams N_s is the same for all the UEs.

into the term \mathbf{i}_k^p . It is straightforward to verify that, when there are no antenna calibration errors (i.e., when $\tilde{\mathbf{G}}_{k,l}^{\text{DL}} = [\tilde{\mathbf{G}}_{k,l}^{\text{UL}}]^H$), the useful term in (5) simplifies to $(N_{UE}/N_s) \sum_l a_{k,l} \sqrt{\rho_{k,l}} \mathbf{s}_k^p$, which is thus proportional to the data vector to be estimated. In the more realistic scenario where calibration errors occur, (5) instead indicates that the data vector \mathbf{s}_k^p is premultiplied by a non-diagonal mixing matrix, which significantly degrades the overall system performance. In particular, assuming that the antenna arrays at the APs are perfectly calibrated⁴, i.e. that $\Phi_{rx,l}^{\text{AP}}$ and $\Phi_{tx,l}^{\text{AP}}$ are identity matrices, for any l , the true UL and DL channels reduce to $\tilde{\mathbf{G}}_{k,l}^{\text{UL}} = \mathbf{G}_{k,l} \tilde{\Phi}_{tx,k}^{\text{UE}}$ and $\tilde{\mathbf{G}}_{k,l}^{\text{DL}} = \tilde{\Phi}_{rx,k}^{\text{UE}} \mathbf{G}_{k,l}^H$, respectively. Substituting these expressions into (5) and applying the identity $[(\tilde{\Phi}_{tx,k}^{\text{UE}})^H \mathbf{A}_{k,l} \tilde{\Phi}_{tx,k}^{\text{UE}}]^{-1} = (\tilde{\Phi}_{tx,k}^{\text{UE}})^{-1} \mathbf{A}_{k,l}^{-1} (\tilde{\Phi}_{tx,k}^{\text{UE}})^{-H}$, with $\mathbf{A}_{k,l} = \mathbf{G}_{k,l}^H \mathbf{G}_{k,l}$, the useful term in (5) becomes

$$\sum_{l=1}^L a_{k,l} \sqrt{\rho_{k,l}} \mathbf{M}_k^H \tilde{\Phi}_{rx,k}^{\text{UE}} [\tilde{\Phi}_{tx,k}^{\text{UE}}]^{-H} \mathbf{M}_k \mathbf{s}_k^p, \quad (6)$$

where $(\cdot)^{-H}$ denotes the Hermitian inverse. It is thus seen that the data vector \mathbf{s}_k^p is pre-multiplied by a diagonal matrix whose entries depend on the unknown matrices $\tilde{\Phi}_{rx,k}^{\text{UE}}$ and $\tilde{\Phi}_{tx,k}^{\text{UE}}$, and that, for each data stream, combine in a non-coherent way the contributions coming from the (N_{UE}/N_s) antennas reserved to that stream. In the following, we show how the use DSTBC can be properly introduced in our system so as to perform data detection without knowing $\tilde{\Phi}_{rx,k}^{\text{UE}}$ and $\tilde{\Phi}_{tx,k}^{\text{UE}}$.

III. DSTBC-BASED DL DATA TRANSMISSION

DSTBC extends classical STBC by transmitting multiple copies of a users data symbols across antennas and time, encoding them into structured spacetime codewords. The receiver recovers the data from phase differences between successive codewords, thus obtaining transmit diversity without requiring instantaneous channel state information. In [8], the authors showed how DSTBC can address AP phase misalignments in joint coherent DL data transmission for single-antenna UEs. In this letter, we instead use DSTBC to handle UE-side antenna calibration errors. We propose a transmission scheme that removes the need to calibrate UE antennas and mitigates distortions from the UEs RF chains. We also design the differential encoding, transmission, and data detection to properly combat UE-side antenna calibration errors.

A. Differential Encoding and Transmission

Consider an arbitrary UE k served by a subset of APs denoted by \mathcal{L}_k , with $L_k = |\mathcal{L}_k|$ being the number of APs serving this UE. Let P represent the number of symbol periods spanned by each space-time codeword. Recalling that N_s parallel data streams are intended for UE k , denote by $\{\mathcal{S}_{k,j}\}_{j=1}^{N_s}$ the collection of symbol sequences for these streams. Specifically, the j th data stream consists of the sequence $\mathcal{S}_{k,j} = \{s_{k,j}^1, s_{k,j}^2, \dots, s_{k,j}^{N_{\text{sym}}}\}$, where N_{sym} is the total number of complex symbols for stream j , each drawn from a *unitary* constellation. The central processing unit (CPU)

⁴In practice, AP arrays are not perfectly calibrated. In this letter, we assume perfectly calibrated APs to isolate the effects of UE-side calibration errors. AP calibration procedures are available in, e.g., [3], [4].

splits each stream $\mathcal{S}_{k,j}$ into smaller segments of n_s symbols each. Denoting by τ_d the length in discrete samples of the channel coherence time devoted to data transmission, we let $G = \lfloor \tau_d/P \rfloor - 1$ denote the number of such segments within the τ_d data-symbol duration, so that $N_{\text{sym}} = (G - 1)n_s$. The t -th segment of stream j is denoted by

$$\mathcal{S}_{k,j}^t = \{s_{k,j}^{(t-1)n_s+1}, \dots, s_{k,j}^{tn_s}\}, \quad |\mathcal{S}_{k,j}^t| = n_s, \quad (7)$$

for $t = 1, 2, \dots, G - 1$. Each such symbol segment is then mapped to a space-time code matrix $\mathbf{X}_{k,j}^t \in \mathbb{C}^{L_k \times P}$. For simplicity and without loss of generality, we focus on *square* STBC codewords, i.e., we assume that $L_k = P$. This assumption holds for many standard orthogonal designs.

Once the set of code matrices $\{\mathbf{X}_{k,j}^t\}$ is defined for each data stream j , the CPU performs *differential encoding* across successive codewords. In particular, the CPU generates a sequence of transmit matrices $\{\mathbf{C}_{k,j}^t\}$ by the recursion

$$\mathbf{C}_{k,j}^t = \mathbf{C}_{k,j}^{t-1} \mathbf{X}_{k,j}^t, \quad \mathbf{C}_{k,j}^0 = \mathbf{I}_{L_k}, \quad (8)$$

for each stream $j = 1, \dots, N_s$. The matrix $\mathbf{C}_{k,j}^t \in \mathbb{C}^{L_k \times L_k}$ represents the encoded information to be transmitted to UE k on stream j during the t -th codeword interval. To this aim, the proposed scheme assumes that each row of $\mathbf{C}_{k,j}^t$ is assigned to one of the APs serving UE k . Since the APs have their own indexing, we define a mapping function $m(l, k)$ that maps each actual AP index $l \in \mathcal{L}_k$ to a row index in $\{1, \dots, L_k\}$. Before transmission, the CPU uses this mapping to distribute the rows of $\mathbf{C}_{k,j}^t$ to the appropriate APs. Specifically, the row of $\mathbf{C}_{k,j}^t$ assigned to AP l (where $l \in \mathcal{L}_k$) is given by⁵

$$\mathbf{c}_{k,l,j}^t = [\mathbf{C}_{k,j}^{t-1}]_{m(l,k),:} \mathbf{X}_{k,j}^t, \quad (9)$$

which is a $1 \times L_k$ row-vector. In other words, AP l (the $m(l, k)$ -th serving AP for UE k) will transmit the row $\mathbf{c}_{k,l,j}^t$ of the new code matrix $\mathbf{C}_{k,j}^t$ for each stream j . The collection of signals to be sent by AP l to UE k (across all streams) can be gathered into an $N_s \times L_k$ matrix

$$\mathbf{B}_{k,l}^t = [(\mathbf{c}_{k,l,1}^t)^T \dots (\mathbf{c}_{k,l,N_s}^t)^T]^T, \quad (10)$$

which stacks the transmit row-vectors for streams $1, \dots, N_s$. The l -th AP then precodes and transmits the signal blocks $\mathbf{B}_{k,l}^t$ to the UE k using the beamformer $\mathbf{W}_{k,l} \in \mathbb{C}^{N_{\text{AP}} \times N_{\text{UE}}}$ introduced in the previous section. The signal received by UE k over the t -th codeword interval is thus expressed as

$$\mathbf{Y}_k^t = \sum_{l \in \mathcal{L}_k} \tilde{\mathbf{G}}_{k,l}^{\text{DL}} \mathbf{W}_{k,l} \mathbf{M}_k \mathbf{B}_{k,l}^t + \mathbf{N}_k^t, \quad (11)$$

where $\mathbf{N}_k^t \in \mathbb{C}^{N_{\text{UE}} \times L_k}$ in (11) is the combined interference-plus-noise matrix at UE k during the t -th codeword interval. The key challenge is that UE k does not know the effective channel $\tilde{\mathbf{G}}_{k,l}^{\text{DL}} \mathbf{W}_{k,l} \mathbf{M}_k$ in (11); this motivates a differential detection approach, as described next.

B. Differential Detection at the Receiver

At UE k , the goal is to detect the transmitted code matrices $\mathbf{X}_{k,j}^t$ without knowing the instantaneous channel phases. To do so, we assume that the unknown offset matrices $\tilde{\Phi}_{tx,k}^{\text{UE}}$

and $\tilde{\Phi}_{rx,k}^{\text{UE}}$ remain approximately *constant*⁶ over at least two consecutive codeword intervals. Under this assumption, the effective channel matrices for intervals t and $t-1$ are basically the same. Thus the channel effects cancel out when processing \mathbf{Y}_k^t and \mathbf{Y}_k^{t-1} differentially, as briefly illustrated in Appendix B. Because multiple data streams are transmitted (one per UE antenna group), the N_{UE} antennas at UE k observe a superposition of all streams. From (6), each stream is received over (N_{UE}/N_s) antennas. Thus, the N_{UE} antennas can be conceptually divided into N_s groups of $N_b = N_{\text{UE}}/N_s$ antennas, each mainly corresponding to one stream. To separate the streams, UE k partitions the received signal matrix \mathbf{Y}_k^t by grouping its rows per stream. In particular, the portion of \mathbf{Y}_k^t carrying stream j is obtained by extracting the rows associated with the j -th antenna group. We denote this sub-matrix as

$$\tilde{\mathbf{Y}}_{k,j}^t \triangleq [\mathbf{Y}_k^t]_{(j-1)N_b+1:jN_b, :}, \quad (12)$$

for $j = 1, \dots, N_s$, where the notation $[\cdot]_{a:b, :}$ indicates we take rows a through b of \mathbf{Y}_k^t (and all columns). An analogous definition gives $\tilde{\mathbf{Y}}_{k,j}^{t-1}$ from \mathbf{Y}_k^{t-1} . After this stream-wise separation, each $\tilde{\mathbf{Y}}_{k,j}^t$ is an $N_b \times L_k$ matrix containing the received superimposed codeword for stream j (from all L_k serving APs) over the $P = L_k$ symbol periods.

Finally, assuming that phase-shift keying (PSK) modulation is employed, the detection of $\mathbf{X}_{k,j}^t$ can be performed using the following maximum likelihood (ML) criterion [9]

$$\hat{\mathbf{X}}_{k,j}^t = \arg \max_{\mathbf{X} \in \mathcal{X}_N} \text{Re}\{\text{tr}\{\mathbf{X} (\tilde{\mathbf{Y}}_{k,j}^t)^{\text{H}} \tilde{\mathbf{Y}}_{k,j}^{t-1}\}\}, \quad (13)$$

where \mathcal{X}_N is the set of all possible code matrices for a given unitary constellation \mathcal{S} . In (13), $\text{Re}\{\cdot\}$ denotes the real part, and $\text{tr}\{\cdot\}$ is the matrix trace. This criterion compares the correlation between the received signal blocks $\tilde{\mathbf{Y}}_{k,j}^t$ and $\tilde{\mathbf{Y}}_{k,j}^{t-1}$ with each candidate code matrix \mathbf{X} in the codebook, and selects the one that best matches. Although the product $(\tilde{\mathbf{Y}}_{k,j}^t)^{\text{H}} \tilde{\mathbf{Y}}_{k,j}^{t-1}$ may introduce multi-user interference cross-terms, their impact is reduced by the adopted precoding techniques. The entire outlined procedure is summarized in Algorithm 1.

C. Complexity Analysis and System Overhead

The proposed scheme adds complexity from differential encoding at the CPU and data detection at the UE (see Algorithm 1). At the CPU, (8) requires one $L_k \times L_k$ matrix multiplication per stream, i.e., L_k^3 complex multiplications. Since L_k is typically small (e.g., $L_k \leq 4$), this cost is negligible compared to the precoding overhead in coherent transmission.

At the UE, the main operations are: (i) computing $(\tilde{\mathbf{Y}}_{k,j}^t)^{\text{H}} \tilde{\mathbf{Y}}_{k,j}^{t-1}$, requiring $N_b L_k^2$ complex multiplications per stream; and (ii) the codebook search. Although the codebook has size M^{N_s} , the orthogonality of the code matrices allows symbol-wise decoding, reducing complexity from $\mathcal{O}(M^{N_s})$

⁶This assumption is practical because phase offsets from calibration impairments change much more slowly than baseband symbols and are thus quasi-static over two differential blocks. For example, 5G NR symbols last tens of microseconds, whereas hardware offsets typically vary over milliseconds or longer.

⁵Eq. (9) remains valid if $L_k < P$. For instance, in a configuration with $L_k = 3$ and $P = 4$, the CPU does not assign the last row of $\mathbf{C}_{k,j}^t$ to any AP, as Eq. (9) maps the rows of $\mathbf{C}_{k,j}^t$ only to the APs serving the UE.

Algorithm 1: DSTBC-based DL Data Transmission

Input: $N_s, G, t = 1, \dots, G-1, k = 1, \dots, K$;
 // Processing at the CPU
 1 The CPU receives $\{\mathcal{S}_{k,j}\}_{j=1}^{N_s}$; // Parallel data streams
 2 **for** $j = 1$ **to** N_s **do**
 3 Split $\mathcal{S}_{k,j}$ into segments $\mathcal{S}_{k,j}^t$ in (7);
 4 Map $\mathcal{S}_{k,j}^t$ onto a space-time code matrix $\mathbf{X}_{k,j}^t$;
 5 Differential encoding: $\mathbf{C}_{k,j}^t = \mathbf{C}_{k,j}^{t-1} \mathbf{X}_{k,j}^t$ in (8);
 6 Assign the rows of $\mathbf{C}_{k,j}^t$ to the serving APs via (9);
 7 **end**
 8 Build $\mathbf{B}_{k,l}^t$ in (10) and forward it to the serving APs;
 9 The serving APs transmit $\mathbf{B}_{k,l}^t$ to UE k ;
 // Data detection at the UE
 10 UE k receives the aggregate DL signal \mathbf{Y}_k^t in (11);
 11 **for** $j = 1$ **to** N_s **do**
 12 Extract $\tilde{\mathbf{Y}}_{k,j}^t$ and $\tilde{\mathbf{Y}}_{k,j}^{t-1}$ from \mathbf{Y}_k^t and \mathbf{Y}_k^{t-1} in (12);
 13 Detect $\hat{\mathbf{X}}_{k,j}^t$ via (13), i.e., $\hat{\mathbf{X}}_{k,j}^t$;
 14 **end**
Output: $\hat{\mathbf{X}}_{k,j}^t$

to $\mathcal{O}(N_s M)$. Thus, as in coherent detection, the overall complexity stays linear in the constellation size [9].

IV. NUMERICAL RESULTS

Unless stated otherwise, we consider a CF-mMIMO network comprising $K = 20$ UEs and $L = 40$ APs. The UEs are equipped with $N_{\text{UE}} = 2$ antennas, while each AP has $N_{\text{AP}} = 8$ antennas. Each UE receives $N_s = 2$ simultaneous data streams. The UEs are uniformly distributed within a 0.5×0.5 km² area, while the distribution of APs follow a hard core point process (HCPP)⁷. The entries of the matrices $\tilde{\Phi}_{tx,k}^{\text{UE}}$ and $\tilde{\Phi}_{rx,k}^{\text{UE}}$ are assumed to have unit modulus and uniformly distributed phase, for any k . Besides the ZISI precoder, also the partial MMSE (P-MMSE) precoder, described in Appendix A, is used for the numerical results. We consider a channel coherence block of discrete length $\tau_c = 200$; of these $\tau_p = 16$ samples are used for UL training, and $\tau_d = 184$ for DL transmission. The total transmit powers per UE and per AP are set to 100 mW and 200 mW, respectively.

To evaluate the BER and SE, Monte Carlo simulations are performed to account for different channel realizations and AP/UE locations, referred to as setups. The SE for UE k in each setup is calculated as

$$\text{SE}_k = P_f \log_2(M_o) (1 - \mathbb{E}\{\text{BER}_k\}) \quad (14)$$

where $M_o = 8$ is the modulation order, and $\mathbb{E}\{\text{BER}_k\}$ denotes the average BER computed over all channel realizations. P_f is the usual pre-log factor; specifically, $P_f = \tau_d/\tau_c$ for conventional CF-mMIMO, and $P_f = (G-1)n_s/\tau_c$ for CF-mMIMO employing DSTBC, with $G = \lceil \tau_d/L_k \rceil$. Let $\mathcal{K}_l \subset \{1, \dots, K\}$ denote the subset of UEs served by AP l . In distributed processing, the power allocated to UE k regarding AP l is given by $\rho_{k,l} = \rho_{k,l}^{\text{norm}} (\sqrt{\beta_{k,l}} / \sum_{k' \in \mathcal{K}_l} \sqrt{\beta_{k',l}})$,

⁷This approach enforces a minimum distance of $d_{\min} = \sqrt{A/L}$ between any two APs, where A denotes the coverage area.

where $\rho_{k,l}^{\text{norm}} = \rho_{\max} / \|\mathbf{W}_{k,l}^{\text{ZISI}}\|_F^2$ and $k \neq k'$. In the centralized one, the power coefficient ρ_k is computed as [6], [10]

$$\rho_k = \frac{\rho_{\max}}{\rho_k^{\text{norm}}} \frac{\left(\sum_{l \in \mathcal{L}_k} \beta_{k,l}^\zeta \right)^\kappa}{\max_{\ell \in \mathcal{L}_k} \sum_{i \in \mathcal{K}_\ell} \left(\sum_{l \in \mathcal{L}_i} \beta_{i,l}^\zeta \right)^\kappa}, \quad (15)$$

where $\rho_k^{\text{norm}} = \sum_{l=1}^L \mathbb{E}\{\|\mathbf{W}_{k,l}^{\text{P-MMSE}}\|_F^2\}$, and the operator $\|\cdot\|_F$ represents the Frobenius norm. Moreover, ζ and $\kappa \in [0, 1]$ are design parameters, defined as $\zeta = 0.2$ and $\kappa = 0.5$ [2], [10]. The 3GPP Urban Micro (UMi) path loss model is used to describe the propagation channel. The shadow fading standard deviation is 4 dB; AP and UE antenna heights are 11.65 m and 1.65 m, respectively; the receiver noise figure is 8 dB. The system uses a 3.5 GHz carrier with 20 MHz bandwidth. For AP clustering, we associate each UE with the L_k APs with the strongest channel gains [11], while pilot assignment follows [2].

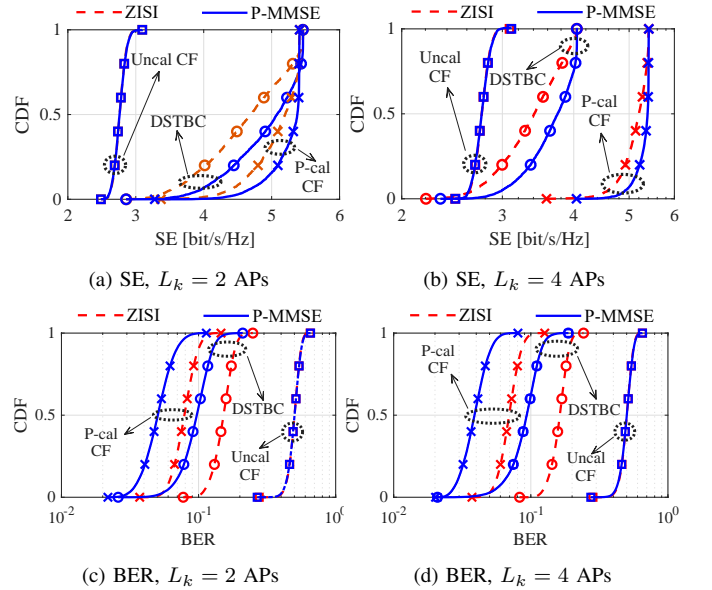


Fig. 2: Cumulative distribution function (CDF) of the average SE and BER for each setup. Here: $L = 40, K = 20, N_{\text{AP}} = 8, N_{\text{UE}} = 2$, and $N_s = 2$.

Fig. 2 shows the CDFs of the average BER and SE for perfectly calibrated (P-cal) and uncalibrated (Uncal-CF) CF-mMIMO systems, compared with the proposed approach (DSTBC) under both ZISI and P-MMSE precoding. Phase offsets from the UE antennas degrade the BER and SE of CF-mMIMO systems with coherent DL transmission. In the uncalibrated case, P-MMSE and ZISI perform similarly because UE-side phase offsets break channel reciprocity, preventing accurate interference mitigation and phase alignment. In the DSTBC-based scheme, P-MMSE still outperforms ZISI thanks to better interference suppression, which helps the proposed method counteract the unwanted cross-product effects in (13). However, the SE gain decreases for $L_k > 2$ due to the DSTBC pre-log factor, which depends on the code rate R ($R = 3/4$ for $L_k = 4$) [8]. This reveals an SE/BER trade-off: larger AP clusters improve reliability (BER) via diversity but incur an SE penalty, requiring a careful choice of L_k and the number of data streams.

Fig. 3, finally, shows the average network SE versus the

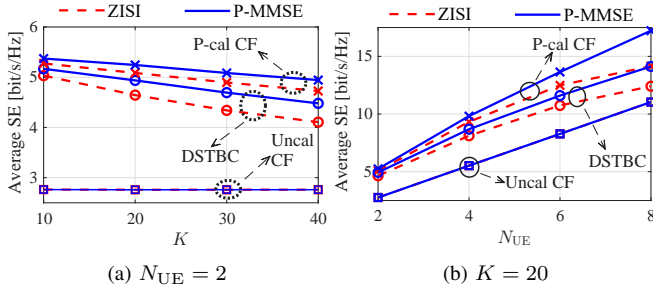


Fig. 3: Average SE as a function of (a) the number of UEs K in the network and (b) the number of antennas per UE, N_{UE} . Here, $L = 40$, $N_{\text{AP}} = 8$, $L_k = 2$, and $N_s = N_{\text{UE}}$.

number of UEs K and antennas per UE N_{UE} . The proposed approach restores the SE of UC CF-mMIMO systems as K and N_{UE} increase, whereas ZISI degrades more with larger K due to weaker interference suppression than P-MMSE. The SE does not grow linearly with N_{UE} because extra data streams increase inter-stream interference and pilot contamination worsens with N_{UE} , limiting SE gains.

V. CONCLUSIONS

This letter introduced a DSTBC-based strategy to mitigate the impact of UE antenna miscalibration in CF-mMIMO systems. Results showed that uncalibrated arrays at the UE degrade BER and SE in conventional setups, while the proposed scheme approaches the ideal calibrated case.

APPENDIX A: THE P-MMSE PRECODER

The P-MMSE precoding technique suppresses interference only to the UEs most strongly affected by the DL transmission to UE k , defined as $\mathcal{P}_k = \{i : \mathbf{a}_k \mathbf{a}_i^H \neq \mathbf{0}_{L \times L}\}$, where $\mathbf{a}_k = [a_{k,1}, \dots, a_{k,L}]^T \in \mathbb{C}^{L \times 1}$. It is obtained from the MMSE formulation in [6], but applied only to the channel estimates of the UEs in \mathcal{P}_k . Denoting the estimated channel matrix of UE i as $\hat{\mathbf{G}}_i^{\text{UL}} = [(\hat{a}_{i,1} \hat{\mathbf{G}}_{i,1}^{\text{UL}})^T, \dots, (\hat{a}_{i,L} \hat{\mathbf{G}}_{i,L}^{\text{UL}})^T]^T \in \mathbb{C}^{LN_{\text{AP}} \times N_{\text{UE}}}$, the P-MMSE precoder is $\mathbf{W}_k^{\text{P-MMSE}} = \sqrt{\rho_k \eta_k} [\sum_{i \in \mathcal{P}_k} \eta_i \bar{\mathbf{W}}_i + \sigma_{\text{UL}}^2 \mathbf{I}_{LN_{\text{AP}}}]^{-1} \hat{\mathbf{G}}_k^{\text{UL}}$ where $\bar{\mathbf{W}}_i = \hat{\mathbf{G}}_i^{\text{UL}} (\hat{\mathbf{G}}_i^{\text{UL}})^H + \mathbf{Z}_{\hat{\mathbf{G}}_i^{\text{UL}}}$, and $\mathbf{Z}_{\hat{\mathbf{G}}_i^{\text{UL}}}$ is the covariance of the estimation error $\mathbf{G}_i^{\text{UL}} = \hat{\mathbf{G}}_i^{\text{UL}} - \hat{\mathbf{G}}_i^{\text{UL}}$, i.e., $\mathbf{Z}_{\hat{\mathbf{G}}_i^{\text{UL}}} = \mathbb{E}\{\mathbf{G}_i^{\text{UL}} (\mathbf{G}_i^{\text{UL}})^H\}$. Here, ρ_k is the total power allocated to UE k , η_k is its per-antenna transmit power, and σ_{UL}^2 is the UL noise variance.

APPENDIX B: UE CALIBRATION ERROR MITIGATION

We now give a simplified analytical example under specific assumptions to show how DSTBC schemes mitigate UE-side antenna calibration errors. Assuming perfect channel estimates at the APs, a ZISI precoder, and perfectly calibrated AP antenna arrays (i.e., $\Phi_{r,l}^{\text{AP}} = \Phi_{t,l}^{\text{AP}} = \mathbf{I}_{N_{\text{AP}}}$), and following the same procedure as for (6), Eq. (11) can be rewritten as

$$\mathbf{Y}_k^t = \sum_{l \in \mathcal{L}_k} \sqrt{\rho_{k,l}} \tilde{\Phi}_{r,x,k}^{\text{UE}} [\tilde{\Phi}_{t,x,k}^{\text{UE}}]^{-H} \mathbf{M}_k \mathbf{B}_{k,l}^t + \mathbf{N}_k^t. \quad (16)$$

W.l.o.g., assume $N_{\text{UE}} = 4$, $N_s = 2$, and $L_k = 2$. By denoting the indexes of the serving APs as l and l' , the useful term \mathbf{U}_k^t

of \mathbf{Y}_k^t becomes

$$\mathbf{U}_k^t = \begin{bmatrix} \phi_{r,k}^1 (\phi_{t,k}^1)^{-H} \mathbf{c}_{k,l,1}^t \\ \phi_{r,k}^2 (\phi_{t,k}^2)^{-H} \mathbf{c}_{k,l,1}^t \\ \phi_{r,k}^3 (\phi_{t,k}^3)^{-H} \mathbf{c}_{k,l,2}^t \\ \phi_{r,k}^4 (\phi_{t,k}^4)^{-H} \mathbf{c}_{k,l,2}^t \end{bmatrix} + \begin{bmatrix} \phi_{r,k}^1 (\phi_{t,k}^1)^{-H} \mathbf{c}_{k,l',1}^t \\ \phi_{r,k}^2 (\phi_{t,k}^2)^{-H} \mathbf{c}_{k,l',1}^t \\ \phi_{r,k}^3 (\phi_{t,k}^3)^{-H} \mathbf{c}_{k,l',2}^t \\ \phi_{r,k}^4 (\phi_{t,k}^4)^{-H} \mathbf{c}_{k,l',2}^t \end{bmatrix}. \quad (17)$$

To detect stream j at UE k , $\tilde{\mathbf{Y}}_{k,j}^t$ is computed as in (12). We focus now on the useful term of $\tilde{\mathbf{Y}}_{k,j}^t$ and neglect the interference-plus-noise terms $\mathbf{N}_k^t \in \mathbb{C}^{N_{\text{UE}} \times L_k}$ for analytical tractability. Thus, for the first stream ($j = 1$), we can write $\tilde{\mathbf{U}}_{k,1}^t \in \mathbb{C}^{N_b \times L_k}$ from $\tilde{\mathbf{Y}}_{k,j}^t$ as

$$\begin{bmatrix} \phi_{r,k}^1 (\phi_{t,k}^1)^{-H} & 0 \\ 0 & \phi_{r,k}^2 (\phi_{t,k}^2)^{-H} \end{bmatrix} \begin{bmatrix} \mathbf{c}_{k,l,1}^t + \mathbf{c}_{k,l',1}^t \\ \mathbf{c}_{k,l,1}^t + \mathbf{c}_{k,l',1}^t \end{bmatrix} \quad (18)$$

and define $\tilde{\mathbf{U}}_{k,1}^{t-1}$ in a similar manner. By performing $(\tilde{\mathbf{U}}_{k,1}^t)^H \tilde{\mathbf{U}}_{k,1}^{t-1}$, we obtain

$$\begin{bmatrix} \mathbf{c}_{k,l,1}^t + \mathbf{c}_{k,l',1}^t \\ \mathbf{c}_{k,l,1}^t + \mathbf{c}_{k,l',1}^t \end{bmatrix}^H \tilde{\mathbf{A}}_{r,k}^{\text{UE}} \begin{bmatrix} \mathbf{c}_{k,l,1}^{t-1} + \mathbf{c}_{k,l',1}^{t-1} \\ \mathbf{c}_{k,l,1}^{t-1} + \mathbf{c}_{k,l',1}^{t-1} \end{bmatrix}. \quad (19)$$

where $\tilde{\mathbf{A}}_{r,k}^{\text{UE}} = \text{diag}(|\phi_{r,k}^1 (\phi_{t,k}^1)^{-H}|^2, |\phi_{r,k}^2 (\phi_{t,k}^2)^{-H}|^2)$. Since $\mathbf{c}_{k,l,j}^t$ can also be regarded as $\mathbf{c}_{k,l,j}^t = \mathbf{c}_{k,l,j}^{t-1} \mathbf{X}_{k,j}^t$ in (9), the product $(\tilde{\mathbf{U}}_{k,1}^t)^H \tilde{\mathbf{U}}_{k,1}^{t-1}$ becomes

$$\mathbf{X}_{k,1}^t [\mathbf{c}_{k,l,1}^{t-1} + \mathbf{c}_{k,l',1}^{t-1}]^H [\mathbf{c}_{k,l,1}^{t-1} + \mathbf{c}_{k,l',1}^{t-1}] \|\tilde{\mathbf{A}}_{r,k}^{\text{UE}}\|_F^2, \quad (20)$$

where it can be observed that the effects of UE-side antenna calibration errors are effectively mitigated since $\|\tilde{\mathbf{A}}_{r,k}^{\text{UE}}\|_F^2 = (|\phi_{r,k}^1 (\phi_{t,k}^1)^{-H}|^2 + |\phi_{r,k}^2 (\phi_{t,k}^2)^{-H}|^2)$ is constant during the time interval of two consecutive codewords. The same reasoning applies to the second stream ($j = 2$).

REFERENCES

- [1] S. Buzzi, F. Linsalata, E. Moro, and G. Interdonato, "Why user-centric cell-free distributed MIMO systems will be the disruptive 6G technology," *IEEE Communications Magazine*, pp. 1–7, 2026.
- [2] Ö. Demir, E. Björnson, and L. Sanguinetti, *Foundations of User-Centric Cell-Free Massive MIMO*. Foundations and TrendsSM in Signal Processing, 2021, vol. 14, no. 3-4.
- [3] U. Kunnath Ganesan, R. Sarvendranath, and E. G. Larsson, "Beamsync: Over-the-air synchronization for distributed massive MIMO systems," *IEEE Trans. Wireless Commun.*, vol. 23, no. 7, pp. 6824–6837, 2024.
- [4] N. Kolomvakis and other, "Over-the-air amplitude and phase reciprocity calibration for distributed MIMO," in *Proc. IEEE Int. Symp. Pers., Indoor Mobile Radio Commun. (PIMRC)*, 2025.
- [5] S. Buzzi, C. D'Andrea, A. Zappone, and C. D'Elia, "User-centric 5G cellular networks: Resource allocation and comparison with the cell-free massive MIMO approach," *IEEE Trans. Wireless Commun.*, vol. 19, no. 2, pp. 1250–1264, 2020.
- [6] E. B. Kama, J. Kim, and E. Björnson, "Multi-antenna users in cell-free massive MIMO: Stream allocation and necessity of downlink pilots," 2025. [Online]. Available: <https://arxiv.org/abs/2505.02951>
- [7] E. Shi, J. Zhang, H. Du, B. Ai, C. Yuen, D. Niyato, K. B. Letaief, and X. Shen, "RIS-aided cell-free massive MIMO systems for 6G: Fundamentals, system design, and applications," *Proc. IEEE*, vol. 112, no. 4, pp. 331–364, 2024.
- [8] M. M. M. Freitas, S. Buzzi, and G. Interdonato, "Eliminating phase misalignments in cell-free massive MIMO via differential transmission," *IEEE Wireless Commun. Lett.*, pp. 1–1, 2025.
- [9] E. G. Larsson and P. Stoica, "Space-time block coding for wireless communications," *Cambridge University Press*, 2003.
- [10] S. Chen, J. Zhang, E. Björnson, Ö. T. Demir, and B. Ai, "Energy-efficient cell-free massive MIMO through sparse large-scale fading processing," *IEEE Trans. Wireless Commun.*, vol. 22, no. 12, pp. 9374–9389, 2023.
- [11] M. M. M. Freitas *et al.*, "Scalable user-centric distributed massive MIMO systems with restricted processing capacity," *IEEE Trans. Wireless Commun.*, vol. 23, no. 12, pp. 19933–19949, 2024.